ASIA-PACIFIC JOURNAL OF CHEMICAL ENGINEERING
Asia-Pac. J. Chem. Eng. 2012; **7** (Suppl. 1): S62–S70
Published online 8 November 2011 in Wiley Online Library
(wileyonlinelibrary.com) DOI: 10.1002/apj.642

Special theme research article

Optimization of single mixed refrigerant natural gas liquefaction plant with nonlinear programming

Mohd Shariq Khan,[1] *Sanggyu Lee*[2] *and Moonyong Lee*[1]*

[1]*School of Chemical Engineering, Yeungnam University, Gyeongsan 712-749, Korea*
[2]*Gas Plant R&D Center, Korea Gas Corporation, Incheon 406-130, Korea*

Received 27 January 2011; Revised 19 July 2011; Accepted 20 September 2011

ABSTRACT: The liquefaction of natural gas (NG) in a mixed refrigerant (MR) system is an energy-demanding process. Much energy is wasted because of its irreversibilities and its nonoptimal execution. The most important factors affecting this process's performance are the refrigerant's composition and flow rate, the suction and evaporation pressures, and the extent of refrigerant vaporization. They should be adjusted to optimize the overall operation. The adjustment of one of these variables will affect the other because of their highly nonlinear interactions. This work reports the optimization of a single MR (SMR) process of NG liquefaction. The SMR process was modeled in the UniSim Design commercial process plant simulator, and the model was optimized for compression energy with nonlinear programming (NLP) while satisfying constraints. The base case for optimization was selected by mesh searching, and case study demonstrates that NLP can reduce energy use and improve the process's efficiency. © 2011 Curtin University of Technology and John Wiley & Sons, Ltd.

KEYWORDS: optimization; liquefaction; simulation; refrigerant; sequential quadric programming

INTRODUCTION

Because of its clean burning and ability to meet tough environmental requirements, demand for liquefied natural gas (LNG) has increased considerably, and further increases are predicted[1] for the next several years. Natural gas (NG) is often found in remote locations and requires liquefaction to bring it to the world's markets. This can reduce its volume to a 600th of its original, facilitating its transportation. Liquefaction is energy intensive and consumes approximately 30% of the total energy required for the LNG's production. NG is liquefied by exchanging heat with a refrigerant—a mixture that can provide sufficient refrigeration to liquefy NG in the main cryogenic heat exchanger. The mixed refrigerant (MR) is circulated using compressors after its cooling by mechanical refrigeration cycles.

Several NG liquefaction process are available for base-load LNG plants.[2] C3MR developed by Air Products & Chemicals, Inc. (APCI) accounts for approximately 81% of the world's baseload LNG production capacity. It uses two main cycles, propane precooling to precool the NG and mixed refrigeration to subcool the process stream to approximately −160 °C. A train capacity of 5 Metric Tons Per Annum (MTPA) is possible by the C3MR process. Phillips Optimized Cascade Process uses three pure refrigerants in a cascading series. This process is simple to operate, as pure components minimize the risk of two-phase flow. Also, the loss of one train does not cause the plant shutdown, because production can continue at reduced capacity. This process's facilities can easily shift from LNG recovery to liquefied petroleum gas recovery. Axens' Liquefin™ involves two MR cycles and uses less main equipment. This process maintains efficiency over a wide production range. The AP-X™ Hybrid LNG process developed by Air Products[3] has a possible train capacity of 8 MTPA. Black & Veatch's PRICO is a single MR (SMR) process and has the lowest capital cost of all the competing technologies. APCI's C3MR is the dominant technology and is the most energy efficient over its two refrigeration cycles.[4] SMR processes involve small-scale liquefaction and are the simplest available. Up to 1.3 MTPA LNG capacity is possible. A comparison of available process by energy analysis found SMR the most efficient with respect to energy consumption per kilo mole of LNG per hour and the equipment required.[5,6]

Most liquefactions use MRs, because they can perform better than individual refrigerants.[7] This is because they condense and evaporate over a temperature range and not at a fixed temperature such as single refrigerants.[8] MRs have to undergo cycles of compression, cooling, and expansion to provide refrigeration. Much energy is wasted during liquefaction because of its irreversibility and nonoptimal execution. Prospective energy savings

**Correspondence to*: Moonyong Lee, School of Chemical Engineering, Yeungnam University, Gyeongsan 712-749, Korea. E-mail: mynlee@ynu.ac.kr

are considerable. The most important factors affecting liquefaction's performance are the refrigerant's flow rate and composition and the suction and evaporation pressures. These variables were adjusted in this work to optimize the overall operation. Complications come from the variable's highly nonlinear interactions that greatly affect each other. While adjusting these parameters, constraints were imposed to ensure feasible solutions.

Several methods of optimizing MR systems have been developed. With consideration to the environment, less environmentally damaging refrigerant mixtures have been found using mathematical programming.[9] This involved solving an mixed-integer nonlinear programming (MINLP) model for the target properties of the MR that included environmental factors as constraints. MR was found to have better properties than single refrigerant. Another approach developed for MR systems, which uses nonlinear programming (NLP) and thermodynamics, solves an NLP problem by exploiting the composite curves (CCs) and adjusting refrigerant composition.[10] The SMR process was optimized using graphical targeting in this method; the main loss of energy in liquefaction was found to be associated with the LNG heat exchanger. MR systems have many local optima that required the development of another method to overcome.[11] This involves the NLP being solved by a genetic algorithm, and the objective function was designed with flexibility, incorporating compressor power, minimum total cost, and minimum capital investment so that the objective function could be changed according to the purpose of the design. Another similar optimization of SMR processes used energy consumption as the objective function and was solved by Genetic Algorithm (GA).[12] The enhanced value of some key parameters suggested the cause of the low irreversibility. In all of the mentioned methods, the most demanding part of the optimizations was preparing the objective functions; a lot of time has been spent on it.

With the development of general-purpose process simulators with graphical user interfaces such as Aspen's Hysys and Honeywell's UniSim, processes can be more rigorously modeled and with less effort. The SMR process was modeled by the commercial simulator, UniSim Design (V.R390). Then, by exploiting the COM functionality of UniSim Design, it was connected to Mathwork's MATLAB. This allowed use of the optimization toolbox already provided by Mathwork. The simulator was run through MATLAB subject to its constraints for different algorithms, including fmincon—an NLP-based optimization algorithm. The connection with MATLAB allowed more transparency regarding debugging and troubleshooting. In this study, the MATLAB function fmincon was used to optimize the variables as it can handle both equality and inequality constraints along with the other algorithms provided within the optimization toolbox. Optimization results showed that NLP algorithm can save the energy and improve the process's efficiency provided it starts from a feasible point and searches near the optimum point.

PROCESS DESCRIPTION

The SMR is the simplest NG liquefaction process. An SMR-based plant was first used in 1981 in Skikda, Algeria, where it was installed under license from Pritchard. The SMR process flow sheet is illustrated in Fig. 1. It has four compressor stages and four after coolers. An LNG exchanger and process and refrigerant streams with throttle valves for both streams were installed. The refrigerant is compressed and cooled until liquid and then vaporized in the LNG exchanger over a temperature range. The vaporizing refrigerant takes its latent heat of vaporization from the NG in the LNG exchanger, cooling and, eventually, liquefying the NG. Four compression stages and four intercoolers were used, with compression ratios never exceeding 1 : 3 to prevent power consumption being too high and decreasing the reversibility of the process. The main irreversibility in the SMR process is attributed to the LNG heat exchanger. Fixing the heat exchanger area still allows variation of the refrigerant composition to improve the process's efficiency and to minimize lost work and irreversibility. The Peng–Robinson equation of states was used in this study because it is well developed and widely recognized.

DEGREE OF FREEDOM ANALYSIS

Degree of freedom (DOF) analysis helps to determine the variables needed to be specified to execute a simulation. In steady-state simulation, DOFs are the number of variables (N_V) that must be assigned to solve the nonlinear algebraic system describing the operation unit and are defined as follows:

$$DOF = N_V - N_E \quad (1)$$

The refrigeration part of the SMR process forms a closed recycle loop with several streams interconnected between the units. Thus, the total DOF of the flow sheet was calculated by modifying the formula[13] as follows:

$$DOF = \sum_{i=1}^{U} d_i - (k-1)(N_C + 2) - 2 \quad (2)$$

where d_i represents the DOF of unit; N_C, number of components; and k, the number of interconnecting streams in the refrigeration loop, each one with $(N_C + 2)$ specifications.

The DOF for each unit in the SMR process is shown in Table 1. The LNG exchanger has three process streams

DOI: 10.1002/apj

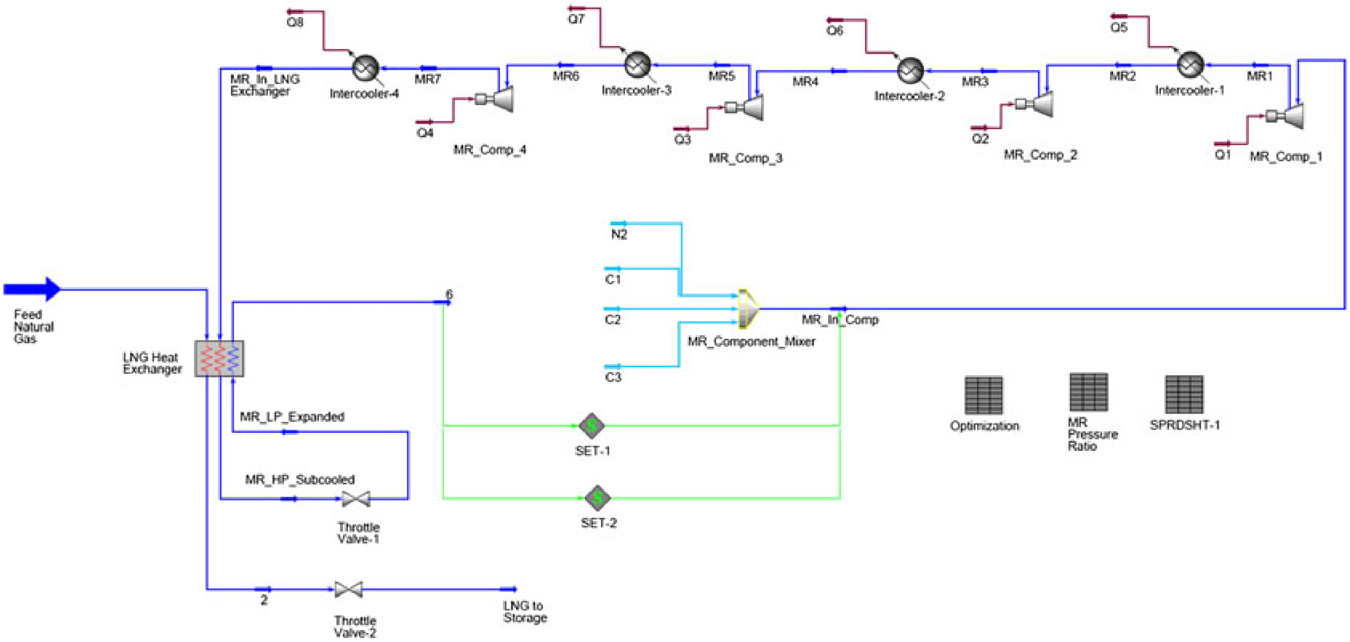

Figure 1. The SMR process model developed in UniSim Design. This figure is available in colour online at www.apjChemEng.com.

exchanging heat: NG stream, hot MR, and cold MR (Fig. 1). Conceptually, the LNG exchanger can be considered as a shell and tube exchanger for calculating associated DOF. NG gas stream is fixed by design parameter. Parameters associated with exchanger geometry such as overall heat transfer coefficient was fixed as a constant based on design parameters. MR outlet temperature and pressure, which correspond to the degree of superheat (see Table 4), were fixed to the values of 36 °C and 1.3 bar as design constraints. Only one dedicated compressor and cooler was used to calculate the DOF for the compressor system as described in the Compressor cooler assembly section. Seawater was used for intermediate cooling of MR, and its outlet was assumed at temperature of 40 °C. Considering all these design factors and constraints, the DOFs of the whole flow sheet are $5(N_C + 2) + 2$, from which we subtract $4(N_C + 2) + 2$ value corresponding to the interconnecting streams. This gives $(N_C + 2)$, where N_C corresponds to the component molar flow rate of MR and one variable in compressor and valve each.

Optimization variables

Several design variables have dominant effects on the performance and efficiency of SMR processes: the refrigerant composition and its flow rate, and the suction and condensation pressures. In MR processes, the refrigerant evaporates and condenses over two different pressure levels. Increasing the difference between these pressure levels prevents temperature crossing in the main LNG exchanger but at the expense of increasing shaft work. There are optimal pressure differences for LNG exchangers that minimize temperature and shaft work. Refrigerant composition is the most flexible and significant variable in the design of MR systems. It is important in avoiding temperature crossing in the LNG exchanger and minimizing shaft work. Refrigerant compositions that have almost parallel CCs while satisfying the minimum internal temperature approach (MITA) are sought. According to the Gibbs phase rule, the number of DOFs of a system having C components, M independent reactions, and Q phase is calculated as follows:

$$F = C - M - Q + 2 \quad (3)$$

Thus, the specification of $C - M - Q + 2$ intensive variables of the individual phases completely fixes the thermodynamic state of each phase. For an MR system of C components, the number of DOFs becomes C, whereas for pure refrigerant systems, the number becomes 1. This advocates that, at a given pressure, the boiling (or dew) temperature of the MR will be a function of the composition, and hence, there are more DOFs than in pure refrigerant system. If the gap between the evaporating and condensing pressure becomes larger, then for pure refrigerant system, the difference in pressure will increase as well, whereas for MR systems, the refrigerant composition can simply be changed while the pressure levels are kept the same. Thus, MR itself

Table 1. Degree of freedom analysis of flow sheet.

Unit	Degree of freedom	Parameters
Compressor	$(N_C + 2) + 1$	P_{out}
Cooler	$(N_C + 2) + 2$	$(P, T)_{outlet}$
Heat Exchanger	$[(N_C + 2) + 2] + [(N_C + 2) + 1]$	$(P,T)_{outlet\ 1}$; $(P)_{outlet\ 2}$
Valve	$(N_C + 2) + 1$	P_{out}

has superior performance than pure refrigerant systems. Moreover, introduction of new component in MR or replacing an existing component by a new one increases the DOF of system, allowing the CC to be designed to avoid temperature cross-problem with decreased shaft work. Optimum refrigerant flow rate also helps in decreasing the irreversibility of the process and consequently in improving its efficiency. Increasing the refrigerant flow rate can widen the gap between the CCs. However, the shaft work requirement also increases. It should be noted if the refrigerant flow rate is too low, it is very difficult, if not impossible, to avoid temperature crosses in the LNG exchanger. Equally, if the refrigerant flow rate is too high, there is a great potential that a certain amount of water exists in the inlet stream to the compressor. Therefore, the refrigerant flow rate can only be changed within a range, and there must exist an optimum flow rate. MR acts as refrigerant for it, inside the LNG exchanger; after being cooled, MR is expanded in a Joule Thompson valve-1 and affects in lowering the temperature. Postexpansion temperature of MR corresponds to its degree of vaporization and is an available DOF. Adjusting the postexpansion temperature allows the variation in degree of vaporization of MR. Lower postexpansion temperature decreases the vapor fraction in MR, which helps in liquefaction of NG but leads to the destruction of pressure energy. On the other hand, higher temperature increases vapor fraction with less destruction of pressure energy. There exists an optimum temperature level, which is sought by numerical optimization. However, comparing to the other variables, this was relatively insensitive

FEED CONDITIONS AND SIMULATION BASIS

The feed conditions used in this work's simulations are listed in Table 2. The commonly used Peng–Robinson Equation of State (EOS) was used to calculate the thermodynamic properties of the MR. The MITA used in the LNG heat exchanger was set at 3 °C, a more conservative approach and which is practically useful. It was also considered that 8% of the NG is converted to Boil off gas (BOG) after the subcooled LNG is flashed to atmospheric pressure, because this amount of gas is sufficient to supply the power required to liquefy the NG.

Compressor cooler assembly

Single MR process is the simplest of all the processes available for NG liquefaction with minimum number of equipment count. The LNG exchanger and the compressor/cooler assembly are the main parts of the process. Only one dedicated compressor is enough for the liquefaction of NG in the SMR process. However, compressors used in industry have a practical maximum stage pressure ratio of around 4–5, it is very common to find compression task performed in multiple stage. In this study, one dedicated compressor, which consists of four stages, was used. Because the intermediate compressors in each stage share a single-power driving axis, the compression ratios between each stage were evenly fixed based on the optimized total compression ratio and thus were not considered as independent optimizing variables.

Table 2. Feed conditions and other assumptions used in simulation.

Property	Condition
NG temperature	32 °C
NG pressure	50 bar
NG flow rate NG composition(mole fraction)	1.0 kg h^{-1}
N_2	0.002000
CH_4	0.913483
C_2H_6	0.053611
C_3H_8	0.021404
n-C_4H_{10}	0.004701
i-C_4H_{10}	0.004601
n-C_5H_{12}	0.000100
i-C_5H_{12}	0.000100
Compressor adiabatic efficiency	0.75
MR temperature after cooler	40 °C
Main Cryogenic Heat Exchanger (MCHE) pressure drop	
ΔP hot stream	1 bar
ΔP cold stream	1 bar

NR, natural gas; MR, mixed refrigerant.

Base case and variable bounds

To better the efficiency of the SMR process by reducing irreversibility, we varied several design parameters within specified bounds. The most significant parameters are the suction and condenser pressures and the refrigerant's composition. The key parameters were bounded based on the prior process knowledge and the process designers' experience. Usually, these bounds were selected from sensitivity analyses. The variables specific constraints can come from their physical nature, e.g. the mole fraction of each component can only be varied between 0 and 1, and from the practicalities of operation, e.g. compression ratios should not exceed 1 : 3. These constraints were applied to all variables with the lower and upper bounds listed in Table 3. The base case parameters of this study were selected by mesh search. This involved exploring a mesh created by the variable bounds by brute force while satisfying the constraints. Objective function and constraints were calculated at every node of the mesh, and feasible solutions were reported. The results of the mesh search depended on the mesh's degree of coarseness, with search times increasing with mesh resolution. By selecting a suitable degree of coarseness, a basic feasible solution was obtained and served as the base case.

Table 3. Variable's limits.

Property	Base case value	Lower bound	Upper bound
N_2 mass flow (kg h^{-1})	0.2510	0.1506	0.3514
CH_4 mass flow (kg h^{-1})	0.5680	0.3408	0.7952
C_2H_6 mass flow (kg h^{-1})	0.5520	0.3312	0.7728
C_3H_8 mass flow (kg h^{-1})	2.930	1.7580	4.6880
Condenser pressure (°C)[†a]	48.00	35	52
MR temperature Postexpansion	−155.0	−162	−152

[a]Suction pressure kept constant and the pressure difference addressed by condenser pressure only.

OBJECTIVE FUNCTION AND CONSTRAINTS

Minimization of total compression power requirements is the objective of this study. In general, the objective function can be defined in relation to the key decision variables by

$$\text{Min } \pounds\ (X) = \sum (Ws + Wcc) \qquad (4)$$

Subject to

$$h_k(X) = 0$$
$$g_k(X) < 0$$
$$c_k < X_k < d_k$$

where X is the key decision variable vector $X = \{ Z_{N2}; Z_{C1}; Z_{C2}; Z_{C3}; \chi; \mu \}$, and Z_{N2} to Z_{C3} denote the mass flows of refrigerant components.

The MR's condensation pressure and postexpansion temperature are represented by χ and μ, respectively. The compression power, *Ws*, was much greater than the power required by the intercooler, *Wcc*, so it can be neglected without any loss of generality. All the physical properties of interest such as bubble point and latent heat of vaporization are included in these variables and constitute the nonlinearity of the process.

Real world design problems frequently encounter constraints posed by the optimization problem that must be satisfied to yield meaningful solutions. In the SMR optimization problem, the MITA of the LNG exchanger and the degree of super heat of the MR must be satisfied. Low MITAs lead to reduced power consumption at the expense of exchanger area, whereas higher MITAs reduce the exchanger area at the expense of operating cost, because more MR must be circulated. A MITA value of 3 °C is a practical solution and was used in this study. The MR's degree of superheat when it leaves the LNG exchanger is also a design constraint; if liquid should enter the compressor, it would have a damaging effect. The outlet temperature of LNG must be −157 °C and is considered a design constraint in this study to liquefy the process stream. The variable bounds are also a type of minimax constraint because they arise from the normal operating range of the equipment to ensure practical design. All design constraints are listed in Table 4.

OPTIMIZATION ALGORITHM

The steady-state optimizer included in the UniSim Design package was first used for the optimization, but because constraint violation problems, the optimization was lifted to MATLAB. The two programs were interfaced by creating an ActiveXcom server. The interface was smooth, allowing efficient information flow between the programs. MATLAB was used for the optimizations because it could easily satisfy constraints and allowed customization of the optimization routine. Their advantages also include detailed output displays and transparency of operation. The popular and robust 'fmincon' optimizer, which uses sequential quadratic programming (SQP), to find minima was used in this study. SQP handles both equality and inequality constraints and solves quadratic programs

Table 4. Design constraints.

Minimax constraints on variable bounds	Design constraints
$0.1506 \le ZN2 \le 0.3514$ (kg h^{-1})	$\Delta T_{min} \ge 3$ °C, minimum internal temperature approach
$0.3408 \le ZC1 \le 0.7952$ (kg h^{-1})	$T_{LNG} \le -157$ °C, exit temperature of LNG from LNG exchanger
$0.3408 \le ZC2 \le 0.7728$ (kg h^{-1})	Degree of superheat of MR = 36 °C
$1.7580 \le ZC3 \le 4.6880$ (kg h^{-1})	
$35 \le \chi \le 52$ (bar)	
$-162 \le \mu \le -152$ (°C)	

DOI: 10.1002/apj

sequentially by minimizing the Lagrangian function with a linear approximation of the constraints. The optimum is defined by the *Karush–Kuhn–Tucker* condition, based on the Lagrange multiplier with inclusion of inequality constraints rather than being restricted to equality constraints. The algorithm used for the optimization of the SMR process is shown in Fig. 2.

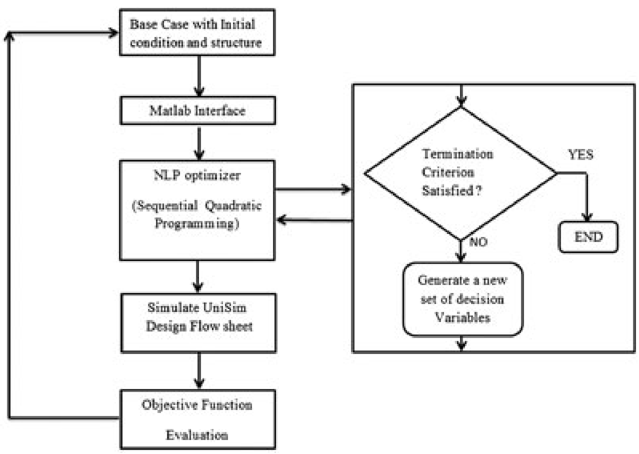

Figure 2. Optimization algorithm.

CONTOUR PLOTS OF OBJECTIVE FUNCTION

Nonlinear programming was used to optimize the SMR process, which is a gradient-based method. To demonstrate the effectiveness of the optimization results, we showed in Fig. 3 the contour plots of objective function evaluation with and without constraints within the minimax bounds. The contour plots show that within the minimax constraints, there are no serious nonlinearities with sharp peaks or narrow valleys that would be problematic to a gradient-based optimizer. Moreover, the SMR process has no recycle or tear streams that may vary between simulation runs and hence validates the use of NLP for this optimization. The dimension of optimization problem is six because we have six optimizing variables. The contour plots shown are based on the variation of two parameters within the minimax bounds and follow the compression energy, whereas the remaining parameters remain constant.

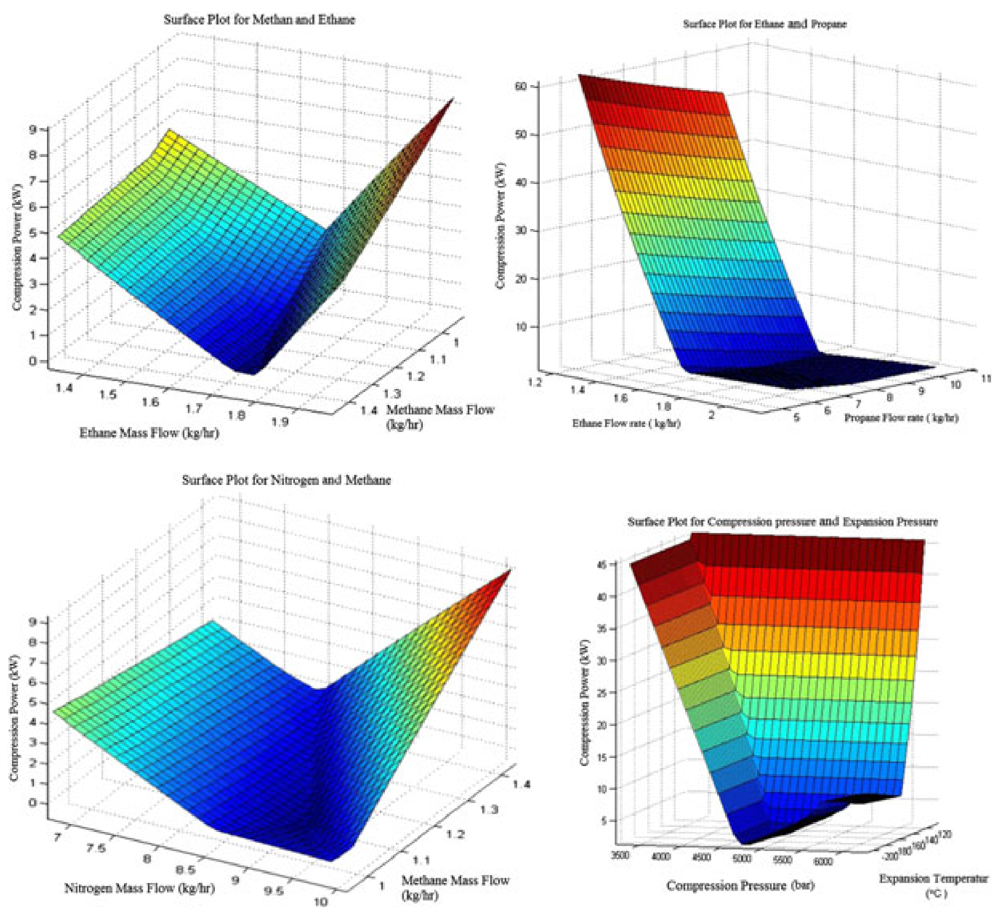

Figure 3. Surface plots of SMR objective function. This figure is available in colour online at www.apjChemEng.com.

Table 5. Thermodynamic first law calculation for the optimized case.

Stream name	Condition	FCp [kJ (h-°C)$^{-1}$]	Tin (°C)	Tout (°C)	H enthalpy (kJ h^{-1})
NG	Hot	2.5462	32	−149.6	462.38
Refrigerant	Cold	–	40	−154.4	462.38

COMPOSITE CURVES

Composite curves are temperature enthalpy diagrams that include the effects of all hot and cold streams. They are important in analyzing the feasibility of optimization results. All the interactions between the variables can be lumped together as hot or cold CCs. They also contain information about the validity of heat transfer.

To construct temperature–enthalpy diagram, the minimum heating and cooling loads have to be first calculated. In NG liquefaction processes, refrigerant is a utility, and the NG feed flow rate and temperature are designed according to the process requirements. Once the cooling load is obtained, the amount of refrigerant (utility) needed can be easily calculated by applying the thermodynamic first law analysis as shown in Table 5. The amount of heat removal for subcooling the NG to −149.6 °C was 462.38 kJ h^{-1}, and the amount of refrigerant was calculated correspondingly.

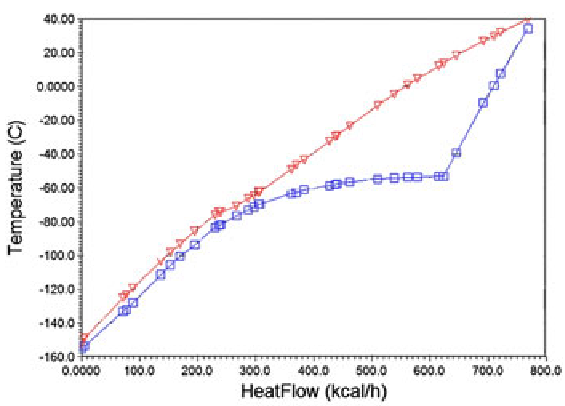

(a) Base case CCs

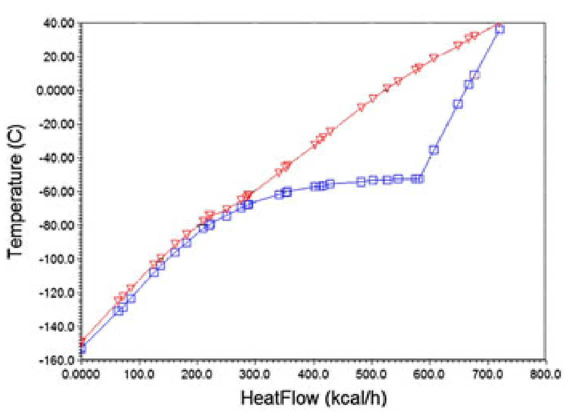

(b) Optimized Case CCs

Figure 4. (a) Base case CCs. (b) Optimized case CCs. This figure is available in colour online at www.apjChemEng.com.

Once the cooling load is calculated, the enthalpy corresponding to the coldest temperature of hot stream (NG) is defined as a base condition: at $T = -149.6$ °C (Fig. 4a), $H = 0$. Next, the cumulative heat available is obtained in the sum of all hot streams as it moves to higher-temperature intervals. The cumulative H *vs* T is plotted, which is the CC for the hot stream as shown in Table 6. Refrigeration is achieved by compressing, cooling, and expanding the MR in a cyclic process. Specific heat requirement of refrigerant changes in the cycle along with the phase change. Calculating enthalpy change of refrigerant along the cycle gives sufficient information for plotting the CC for the cold stream (refrigerant). For instance, refrigerant enters the LNG exchanger in vapor–liquid state and leaves at subcooled state in the first pass. During the second pass, it vaporizes and leaves the exchanger at superheated state. Likewise, following the enthalpy change of refrigerant in the cycle enables plotting the cold CC as shown in Table 7.

Refrigerant exits the LNG exchanger at temperature of 35.43 °C, and the amount of heat flow is 780.2 kcal h^{-1}. The minimum temperature of the refrigerant, which occurs at the stream 'MR_LP_Expanded' in the cycle, was −154.4 °C. At this point, the heat flow is zero because there is no heat transfer between the streams. Different points in the flow sheet have different temperatures and correspondingly different heat flows. The cold CC could be plotted using this information.

The CCs should be MITA apart from each other throughout, with a pinch point at the cold end that gradually opens at higher temperatures. The MR flow, after being evaporated in the heat exchanger, becomes the inlet stream to the compressor. Certain compressors can be

Table 6. Cumulative heat flows of the hot streams for the optimized case.

Temperature (°C)	Heat flow (kcal h^{-1})	Cumulative UA [kJ (°C-h)$^{-1}$]
40.00	749.4	400.9
5.433	565.2	371.5
−45.98	364.0	342.1
−66.30	281.0	287.4
−92.68	166.6	167.1
−151.4	0	0

Table 7. Cumulative heat flows of the clod streams for the optimized case.

Temperature (°C)	Heat flow ($kcal\,h^{-1}$)	Cumulative UA [kJ (°C-h)$^{-1}$]
−154.4	0	0
−102.0	147.8	145.4
−70.07	280.7	287.0
−50.19	523.8	368.1
−37.25	629.5	376.1
2.107	692.5	382.6
35.43	749.4	400.9

Table 8. Optimization results from nonlinear programming.

Objective function	Optimized value	Base case value	Unit
$J = \sum W_s$	0.4244	0.4444	kW
Specific power requirement	1527.82	1600.00	kJ/(kg LNG)$^{-1}$
Manipulated variable	Optimized value	Initial value	Unit
N_2	0.2735	0.2510	$kg\,h^{-1}$
CH_4	0.4630	0.5680	$kg\,h^{-1}$
C_2H_6	0.7176	0.5520	$kg\,h^{-1}$
C_3H_8	2.7470	2.930	$kg\,h^{-1}$
Condenser pressure	47.85	48.00	bar
MR temperature after expansion	−154.4	−155.0	°C

Table 9. Overall performance of liquefied natural gas exchanger for the optimized case.

Performance Parameter	Numerical Value
Overall heat transfer coefficient	399.30 kJ (°C-h)$^{-1}$
Log mean temperature difference	7.852 °C
Duty	3.135e + 03 $kJ\,h^{-1}$

Table 10. Compressor work details for the optimized case.

Compression stage	Pressure (bar)		Power required (kW)
	Inlet	Outlet	
Stage 1	1.300	3.202	0.1122
Stage 2	3.202	7.887	0.1118
Stage 3	7.887	19.43	0.1066
Stage 4	19.43	47.85	0.0936

damaged if the inlet stream contained water. The degree of superheat that accounts for the MR's evaporation is also visible at the hot end of the CC where the cold CC becomes almost a straight line corresponding to the super heat of the MR. The horizontal length of the CCs also gives an idea of the amount of energy required to carry out the task of liquefaction. Horizontal length of the optimized case CC in Fig. 4b is slightly smaller than that of the base case in Fig. 4a, which corresponds to the amount of energy saved by the optimization. In conclusion, the desired hot and cold CCs should be parallel and close to each other, with no temperature cross-occurring for valid heat transfer. The MR should also be superheated at the hot end of the cold CC.

RESULTS AND DISCUSSION

Nonlinear programming optimized the SMR process with respect to key design variables by varying them between fixed bounds while satisfying constraints. The base case for improvement was chosen by mesh searching, and the final optimized values and details of optimization results are listed in Tables 8, 9, and 10. NLP improved the compression energy by approximately 4.5% with respect to the base case. The result's physical meaning is illustrated by the CCs shown in Figs 4a and b, which include the effects of all the hot and cold streams and satisfy the validity of heat transfer. The base case CCs were separated by more than the MITA (3 °C) at the low temperature end where refrigeration is expensive. This gap gave room for improvement. The improvement is visible in the optimized cooling curve, which has the lower end of the CCs closer to each other while sustaining the MITA criterion. This search is gradient based, and the initial solution should be given near to the optimal solution. Fig. 3 shows that optimization did take place near the optimal solution within the minimax bounds and that there are no serious nonlinearities that would affect NLP. The optimization results from NLP were compared with the Multi-star global search method provided in the Matlab optimization toolbox. The Multi-star global search was unable to find a point where the constraints were satisfied. Constraints violation in the Multi-star search can be attributed to its nature because this method invokes the solver from different starting points with no regard for the initial base case. These results indicate that NLP is better for fine tuning results and is successful if optimization commences near the optimal solution.

CONCLUSIONS

Nonlinear programming was used to optimize an NG SMR liquefaction plant. The process was modeled in the commercial simulator, UniSim Design. The base case for optimization was selected by mesh searching, and the optimal result was searched for near the base case with NLP. The optimization proved successful, decreasing the compression energy by 4.5%. This optimization method does not require laborious objective function preparation. Moreover, confidence in the results was given by using a robust model developed in a commercial simulator; the results have more practical significance than those from simplified models. Finally, this method improved the process's efficiency, but because of its deterministic approach, the base case should be considered with proper care, making this method good for fine-tuning results.

Acknowledgements

This research was supported by a grant from the Gas Plant R&D Center funded by the Ministry of Land, Transportation and Maritime Affairs (MLTM) of the Korean government.

REFERENCES

[1] DOE/EIA, Annual Energy Outlook—2010. Energy Information Administration. U.S. Department of Energy, DOE/EIA-0383 (2010), April **2010**.
[2] T. Shukri. LNG Technology Selection. HC Engineering February **2004**.
[3] M.J. Roberts, Y.-N. Liu, J.C. Bronfenbrenner, J. Solomon. Technology Selection. HC Engineering May **2004;** 81–84.
[4] J.M. Geist. *Int. J. Refrig.*, **1983;** *6*(5), 283–297.
[5] C.W. Remeljej, A.F.A. Hoadley. *Energy*, **2006;** *31*(12), 2005–2019.
[6] M.D. Bustan, S. Mahadzi, D. Kharishmadewi. *Asia-Pac. J. Chem. Eng.*, **2011**; 760–770.
[7] N. Churi, L.E.K. Achenie. *Computers & Chemical Engineering*, **1997;** *21*, S349–S354.
[8] S. Vaidyaraman, C.D. Maranas. *Chem. Eng. Comm.*, **2002;** *189*(8), 1057–1078.
[9] A. Duvedi, L.E.K. Achenie. *Comput. Chem. Eng.*, **1997;** *21*(8), 915–923.
[10] G.C. Lee, R. Smith, X.X. Zhu. *Ind. Eng. Chem. Res.*, **2002;** *41*, 5016–5028.
[11] F.D. Nogal, J.-K. Kim, S. Perry, R. Smith. *Ind. Eng. Chem. Res.*, **2008;** *47*, 8724–8740.
[12] M. Mokarizadeh Haghighi Shirazi, D. Mowla. *Energy*, **2010;** *35*, 2878–2885.
[13] A.C. Dimian. *Integrated Design & Simulation of Chemical Processes*, 1st edn edn, Elsevier: Sara Burgerhartstraat 25 P.O. Box 211, 1000 AE Amsterdam, The Netherlands, **2003**.

DOI: 10.1002/apj